

## **THE INFLUENCE OF TEMPERING ON THE MICROSTRUCTURE AND HARDNESS OF “Fe-Mn-Si-Cr-Ni” STAINLESS SHAPE MEMORY STEEL**

Christian Egidio da Silva, [christianegidio@gmail.com](mailto:christianegidio@gmail.com)<sup>1,2</sup>  
Jorge, [jotubo@ita.br](mailto:jotubo@ita.br)<sup>1</sup>

<sup>1</sup>Instituto Tecnológico de Aeronáutica (ITA), 12.228-900, São José dos Campos, SP, Brasil

<sup>2</sup>Gerdau Aços Especiais, 12.442-260, Pindamonhangaba, SP, Brasil

**Abstract.** *The present work was developed to understand the influence of tempering on the microstructure and hardness of “Fe-Mn-Si-Cr-Ni” stainless shape memory steel. Three stainless shape memory steel (Fe-10.3Mn-5.3Si-9.9Cr-4.9Ni-0.006C; Fe-13.7Mn-5.6Si-8.6Cr-5.1Ni-0.014C and Fe-14.2Mn-5.3Si-8.8Cr-4.6Ni-0.008C) were studied varying tempering temperature – 450°C and 620°C (1800s). Microhardness results showed that chemical composition is the most important parameter of influence on hardness – the alloy with higher chromium and lower manganese content presents the highest average hardness. There is a tendency of increasing on hardness with an improving on tempering temperature but not so expressive than the influence of chemical composition. In general, the average hardness presents a tendency to decrease its value with an improvement on austenitizing temperature, suggesting that a higher austenitic grain size conducts to a lower hardness level.*

**Keywords:** *shape memory alloy, stainless steel, heat treatment, tempering, hardness*

### **1. INTRODUCTION**

Since 1990's, Fe-Mn-Si based alloys such as Fe-Mn-Si-Cr-Ni and Fe-Mn-Si-Cr-Ni-Co have been studied as a candidate to substitute Ni-Ti. The Fe-Mn-Si alloys exhibit a nonthermoelastic martensitic  $\gamma(\text{FCC}) \rightarrow \epsilon(\text{HCP})$  transformation and one-way shape memory effect. The martensitic transformation in these alloys is found to proceed by the movement of a/6 112 Shockley partial dislocations on alternate 111 austenite planes. As the shape memory effect mainly results from the reverse motion of Shockley partial dislocations during heating, the martensitic transformation behavior is critical in determining the magnitude of the shape memory effect (Jang et al., 1995).

Due to its lower shape memory effect compared to Ni-Ti, the Fe-Mn-Si based alloys are not employed in large-scale. In order to improve the shape memory effect, the Fe-Mn-Si alloys are submitted to training cycles (thermal mechanical cycling treatment) but that procedure is not viable in several applications. Therefore, it is important to develop materials with good shape memory without the necessity of training.

A good shape memory effect permit to expand the industrial application (Otubo *et al.*, 1997)(Kajiwara, 1999)(Wen *et al.*, 2004)(Jee *et al.*, 2004). According to Li *et al.* (2002) the use of Fe-Mn-Si based alloys is justified by its lower manufacturing cost. In recent years, Fe-Mn-Si based shape memory alloys have received much attention due to the possibility of using them in applications such as pipe joints, bolts, reinforcement of plasters, civil engineering, Seismic vibration and structural aeronautic material (Baruj *et al.*, 2008; Jee et al., 2006; Janke et al., 2005; Otubo et al., 2008; Sawaguchi et al., 2007). In accordance to Verbeken *et al.* (2007), ferrous SMAs based on Fe-Mn alloy system may become a new class of SMAs of great technical importance.

In accordance to Otubo *et al.* (1997; 2008), Jee *et al.* (2004), Sawaguchi *et al.* (2008) and Janke *et al.* (2005), the stainless shape memory alloy can be used in applications such as: pipe joints, electrical connectors, electrical actuators, thermal actuators, vibration damping and external tensioning in civil structures. Works have been done by the group since 1994 to understand the physical metallurgy involved in this material and to permit an optimization on its shape memory recovery capacity (Otubo *et al.*, 1994; 1997; 2002; 2007; 2008)(Nascimento *et al.*, 2000a; 2000b)(Silva *et al.*, 2008a; 2008b; 2008c; 2009). In the earlier works they were shown that beside the chemical composition, the grain size play an important factor in terms of shape recovery performance being higher the smaller the grain size.

### **2. EXPERIMENTAL PROCEDURE**

Three 65mmx65mm ingots were prepared by vacuum induction melting and their chemical composition are shown in Table 1. The ingots were heated to 1,180°C and hot forged down to 40mm x 40mm bars. Then the bars were solution

treated at 1,100°C for 3,600s and then hot rolled to 20mm in diameter round bars. Details regarding its alloy manufacturing process can be found at Otubo *et al* (1994a;1994b;1995).

The 20mm round bars were submitted to austenitizing heat treatment in different temperatures (900°C, 950°C, 1,000°C and 1,050°C) followed by a water quenching. After concluding the quenching they were taken samples of each austenitizing condition and then submitted to a tempering heat treatment. It was used two different tempering conditions: 450°C (30min) and 620°C (30min). The heat treatment (austenitizing and tempering) was performed in a *FCI* furnace model, supplied by *EDG Equipamentos*. The minimum austenitizing temperature used in the present study was 900°C because in the earlier works (Silva *et al*, 2008a;2008b;2008c) it was not observed grain growth up to 900°C. An abrupt grain size increase could be seen for samples austenitized in temperatures between 950°C and 1050°C.

After concluding the tempering, the samples were prepared to perform hardness measurements and metallographic characterization: mechanical grinding (from #320 to #600) followed by a polishing with diamond paste (6µm, 1µm and ¼µm). It was used an optical microscopy *LEICA DMLM* to perform the metallographic analysis.

The hardness evaluation was performed using a *FUTURETECH FM-700* micro hardness tester (0.49N or 50gf, 12s, 10 points per sample in random positions) in accordance to Figure 1. The distance between the different indentations is always higher than 5 times the length of the indentation. It is necessary to clarify this point because it is not recommended to use hardness evaluation if the distance between the different indentations is lower than 3 times the maximum length of the indentation.

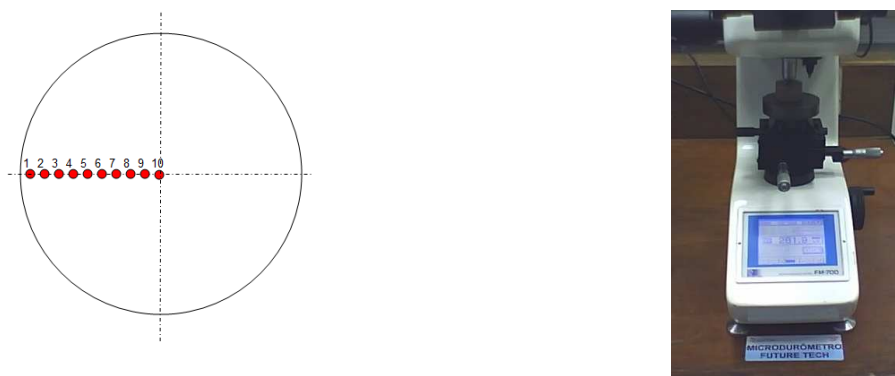


**Figure 1. (a) Scheme of hardness evaluation along the sample radius. (b) Micro hardness equipment used.**

One sample was submitted to an austenitizing at 1200°C, in order to promote a bigger grain growth followed by water tempering at room temperature to “freeze” the microstructures. It was performed hardness evaluation on each phases showed on the microstructure using micro-indentation to know the difference of mechanical characteristics between the phases.

**Table 1. Chemical composition of ingots used in the present study (weight %).**

| ID | Fe      | Mn   | Si  | Cr  | Ni  | C     |
|----|---------|------|-----|-----|-----|-------|
| A  | Balance | 10.3 | 5.3 | 9.9 | 4.9 | 0.006 |
| B  | Balance | 13.7 | 5.6 | 8.6 | 5.1 | 0.014 |
| C  | Balance | 14.2 | 5.3 | 8.8 | 4.6 | 0.008 |

### 3. RESULTS AND DISCUSSIONS

In the earlier works the authors noted that the average austenitic grain size increased almost twice after changing the austenitizing temperature: from 31.70µm (900°C) to 61.90µm (1,050°C). Below 900°C it was not observed any changing on the grain size ending up to 30µm (Silva *et al*, 2008a;2008b;2008c). Figure 2 shows representative microstructures of the studied materials in different austenitizing temperatures (before submitting to tempering). It is possible to note that there is an enormous difference among the microstructures and grain growth is quite visible. All the samples show a heterogeneous microstructure with twins distributed on the austenitic grain.

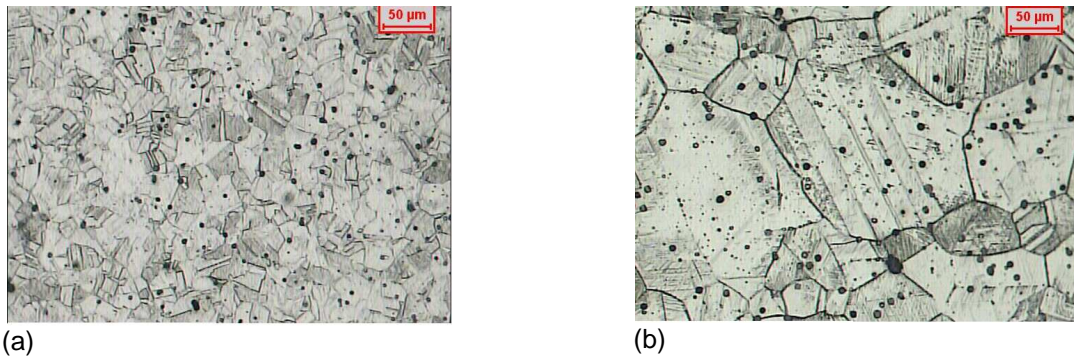


**Figure 2. Representative microstructures of samples submitted to different austenitizing temperatures: (a) 900°C; (b) 1,050°C (Silva *et al*, 2008a;2008b;2008c). Etching: HNO<sub>3</sub> (150 ml) + HF (30 ml) + water (250 ml). Optical microscopy.**

Figure 3 shows a representative microstructure of alloy “A” after submitting to austenitizing at 1,200°C for 2,700s (45min), followed by water quenching (without tempering). It was used a kind of chemical etching which conduct to a differential color between the phases. After hardness scanning (nine measurements by phase) they were found the following results: 255.8 HV ( $\sigma=21.0$ ) for the “dark” phase and 324.3 HV ( $\sigma=12.4$ ) for the “white” phase. In accordance with results obtained by Nascimento *et al* (2008), which studied a similar material, these results suggest that the “dark phase” is austenite and the “white phase” is martensite for the materials studied in the present work.

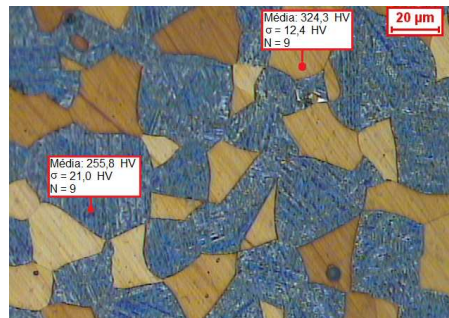


**Figure 3. Representative microstructure of alloy “A” after austenitizing at 1200°C for 2700s. Etching: 1.2g K<sub>2</sub>S<sub>2</sub>O<sub>5</sub> + 0.8g NH<sub>4</sub>HF<sub>2</sub> + 100ml H<sub>2</sub>O. Optical microscopy.**

Figures 4, 5 and 6 show the results of hardness along the radius for the three materials studied in the present work. It is possible to see that alloy “A” presents the highest average hardness among the three chemical compositions. This behavior, in general, was observed for all the austenitizing and tempering temperatures. The average hardness of alloy “B” and “C” are quite similar, suggesting that the difference on the chemical composition observed for alloy “B” and “C” (in accordance with Table 1, “B” presents lower Mn content and higher Ni content than “C”) was not enough to promote relevant changes on the microstructure after submitting the materials to heat treatment.

The legend of graphs permits to know the alloy (“A”, “B” or “C”), the austenitizing temperature (900°, 950°, 1000° or 1050°C) and the tempering condition (450° or 620°C). For example: “B-900-620” means that this test condition is for alloy “B” and this sample was submitted to austenitizing of 900°C followed by a tempering of 620°C.

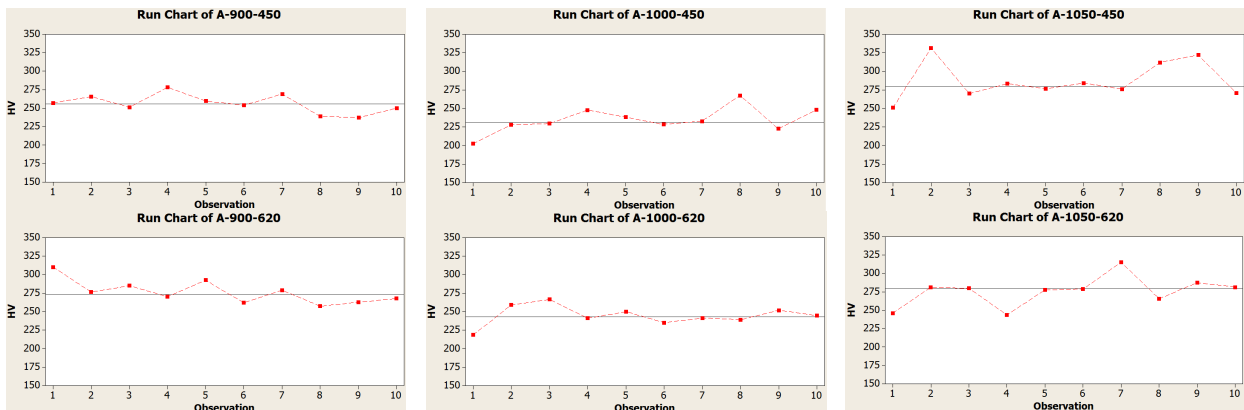


**Figure 4. Hardness results for alloy “A” at different heat treatment temperatures along the sample radius.**

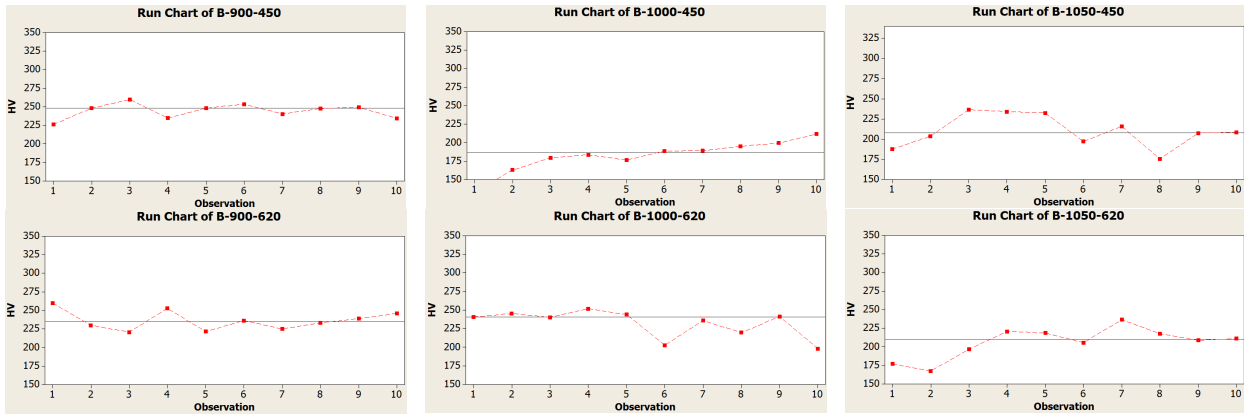


Figure 5. Hardness results for alloy “B” at different heat treatment temperatures along the sample radius.

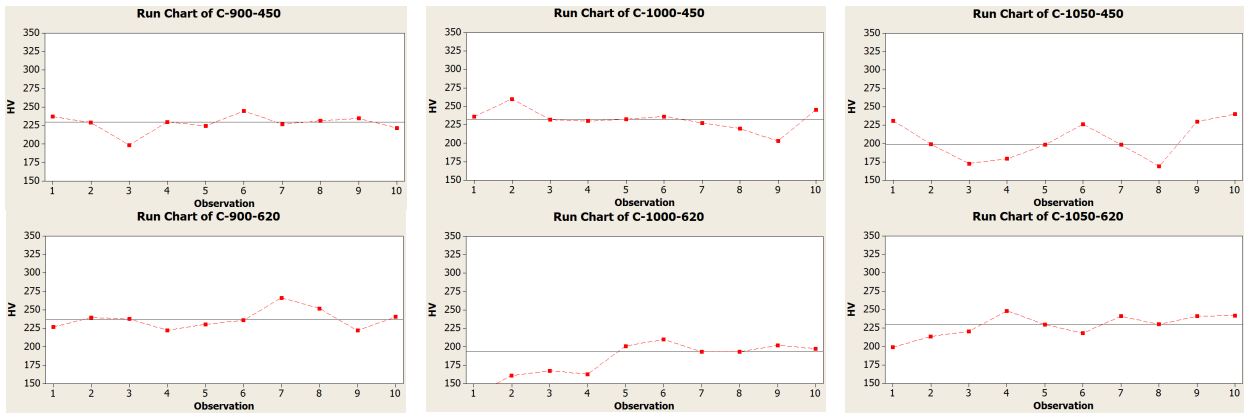


Figure 6. Hardness results for alloy “C” at different heat treatment temperatures along the sample radius.

Analyzing the hardness results as a function of austenitizing temperature (Figures 4 and 5), it is possible to see that the average hardness present a tendency to decrease its value with an improvement on austenitizing temperature ( $\text{Hardness}^{900} > \text{Hardness}^{1000} > \text{Hardness}^{1050}$ ) for alloys “B” and “C”. Alloy “A” (Figure 6) presents a different behavior from 1000°C to 1050°C, but from 900°C to 1000°C it was noted a decreasing on hardness similar to that observed for alloys “B” and “C” (Figures 4 and 5).

Figures 4 suggest that for alloy “A” there is a tendency of increasing on hardness with an improving on tempering temperature. In accordance to Figures 5 and 6, alloys “B” and “C” showed a different behavior: in general the hardness maintain or decrease its values with an increasing on the tempering temperature.

Figure 7 shows the main effects influence of each parameter and the interaction between parameters. These plots were obtained using the statistic software Minitab®.

Analyzing the Figure 7a it is possible to confirm that the average hardness for alloy “B” and “C” (about ~220/230 HV) is quite similar and expressively lower than that noted for alloy “A” (~270 HV). These results confirm the previous comments reported.

In terms of “tempering temperature”, Figure 7a shows that there is no expressive influence of temperature on the overall average hardness. When it is used 620°C there is a little tendency of hardness to increase.

Considering the “austenitizing temperature” (Figure 7a), it is perceived that the highest average hardness level is obtained for 900°C. In general, an increasing on the austenitizing temperature conducted to a decreasing on the hardness, suggesting that a higher austenitic grain size conduct to a lower hardness level.

Analyzing the Figure 7b, it is possible to conclude that there aren’t any interactions among “tempering and austenitizing temperature” or “austenitizing temperature and alloy”.

Excepting to alloy “B”, it can be noted on Figure 7b that an increasing on the “tempering temperature” conducted to a little increasing on the hardness. Alloy “B” presented a little decreasing on the hardness as a function of tempering temperature.

The results of Figure 7b show that the factor “alloy” is the most important parameter. The tempering temperature promotes a little increasing on hardness in general.

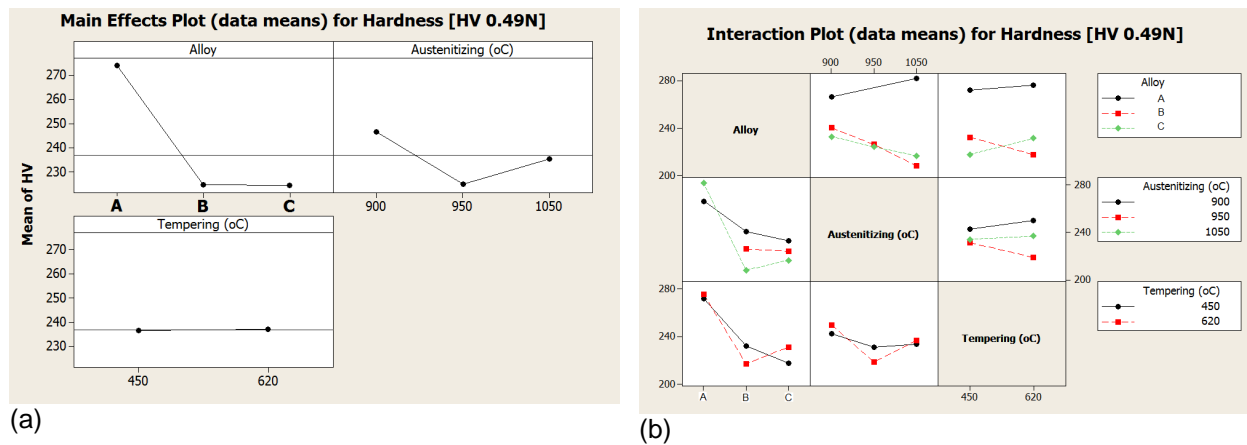


Figure 7. Main effects and interactions plots for alloys “A”, “B” and “C” as a function of austenitizing and tempering temperatures.

Figure 8 shows typical microstructures of alloys “A” and “C” after submitting to tempering in different temperatures. It is possible to see that there is a great difference on the grain size from 900°C to 1050°C of austenitizing temperature. The increasing on the grain size (from 900° to 1050°C) probably conducted to an easy tempering of martensite. This change on the microstructure justifies the decreasing on hardness when the material is submitted to a higher austenitizing temperature.

In accordance to Figure 8 (8c-8b and 8f-8e) the alloy “C” presents a higher plate coarsening than alloy “A”, which can be explained by the difference on the previous grain size of the both material (before submitted to tempering). This feature explains the higher average hardness for alloy “A” in comparison to alloy “C”, as can be shown on Figure 7a.

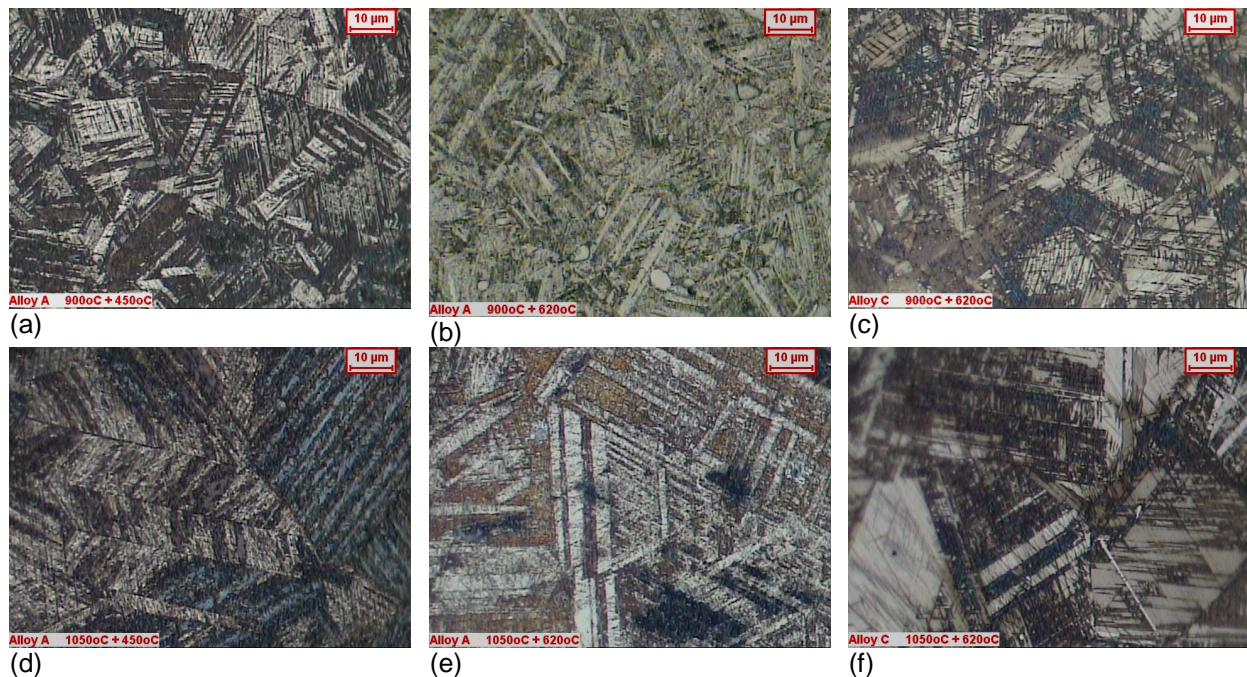


Figure 8. Typical microstructures of alloys “A” and “C” after submitting to tempering in different temperatures. Etching: 1.2g K<sub>2</sub>S<sub>2</sub>O<sub>5</sub> + 0.8g NH<sub>4</sub>HF<sub>2</sub> + 100ml H<sub>2</sub>O. Optical microscopy.

Considering the average hardness obtained to the isolated phases (austenite and martensite), as shown on Figure 3, the both tempering temperatures (450° and 620°C) can be considered efficient to reduce the hardness of material: estimated martensite hardness after quenching of ~324 HV; estimated austenite hardness after quenching of ~255 HV; overall “alloy A” hardness after tempering of 240-260 HV; overall “alloy B/C” hardness after tempering of 220-240 HV. Considering that no relevant difference on hardness on the “as tempered state” was noted comparing 450°C and 620°C, the results suggest that it is not necessary to use a too high temperature to promote a complete tempering.

#### 4. CONCLUSION

Alloy “A” (higher chromium and lower manganese content) presented the highest average hardness. Alloy “B” and “C” presented an average hardness quite similar, suggesting that the difference on the chemical composition observed for alloys “B” and “C” was not enough to promote relevant changes on the microstructures after submitting the materials to heat treatment.

In general, the average hardness presented a tendency to decrease its value with an improvement on austenitizing temperature (hardness 900°C > hardness 1000°C > hardness 1050°C), suggesting that a higher austenitic grain size conduct to a lower hardness level.

There is a tendency of increasing on hardness with an improving on tempering temperature, but that increase did not present an expressive influence on the hardness.

There are not interactions among “tempering and austenitizing temperatures” or “austenitizing temperature and alloy”.

The “chemical composition” seems to be the most important parameter of influence on hardness.

#### 5. REFERENCES

- Baruj, A., Troiani, H.E., 2008, “The effect of pre-rolling Fe-Mn-Si-based shape memory alloys: mechanical properties and transmission electron microscopy examination”, *Materials Science and Engineering A* 481-482, p.574-577.
- Jee, K. K., Han, J. H., Jang, W. Y., 2004, “Measurement of volume fraction of  $\epsilon$  martensite in Fe-Mn based alloys”, *Materials Science and Engineering A* 378, p.319-322.
- Jee, K.K., Han, J.H., Jang, W.Y., 2006, “A method of pipe joining using shape memory alloys”, *Materials Science and Engineering A* 438-440, p.1110-1112.
- Kajiwara, S., 1999, “Characteristic features of shape memory effect and related transformation behavior in Fe-based alloys”, *Materials Science and Engineering A* 273-275, p.67-88.
- Jang, W.Y., Gu, Q., Van Humbeeck, J., Delaey, L., 1995, “Microscopic observation of  $\gamma$ -phase and  $\epsilon$ - and  $\alpha'$ -martensite in Fe-Mn-Si-based shape memory alloys”, *Materials Characterization* 34, p.67-72.
- Janke, L., Czaderski, C. Motavalli, M., Ruth, J., 2005, “Applications of shape memory alloys in civil engineering structures – Overview, limits and new ideas”, *Materials and Structures* 38, p.578-592.
- Li, C. L., Cheng, D. J., Jin, Z. H., 2002, “Influence of deformation temperature on shape memory effect of Fe-Mn-Si-Ni-Cr alloy”, *Materials Science and Engineering A* 325, p.375-379.
- Nascimento, F. C., Rigo, O. D., Otubo, J., Mei, P. R., Moura Neto, C., 2000, “Evolução das fases formadas durante tratamentos termomecânicos em ligas inoxidáveis com efeito de memória de forma”, In: XVII Congresso Brasileiro de Engenharia Mecânica – COBEM, Natal, RN.
- Nascimento, F. C., Otubo, J., Mei, P. R., Cardoso, L. P., 2000, “Determinação das fases  $\gamma$ ,  $\epsilon$  e  $\alpha'$  por difração de raios-X em ligas inoxidáveis com efeito de memória de forma”, In: 55º Congresso Anual da ABM, Rio de Janeiro, RJ.
- Nascimento, F.C., Bueno, J.C., Lepienski, C.M., Otubo, J., Mei, P.R., 2008, “Determinação das propriedades mecânicas da martensita  $\epsilon$  por indentação instrumentada em ligas inoxidáveis com memória de forma”, In: IX Seminário Brasileiro do Aço Inoxidável – INOX'2008, São Paulo, SP. p.65-71.
- Otubo, J., Mei, P. R., Koshimizu, S., 1994, “Desenvolvimento de novos aços inoxidáveis com efeito de memória de forma”, In: IV Seminário Brasileiro do Aço Inoxidável – INOX'94, São Paulo, SP.
- Otubo, J., Mei, P.R., Koshimizu, S., 1994, “Caracterização de aços inoxidáveis com efeito de memória de forma”, In: 11º Congresso Brasileiro de Engenharia e Ciência dos Materiais – CBECiMat, Águas de São Pedro, SP. p.219-222.
- Otubo, J., Mei, P.R., Koshimizu, S., 1995, “Desenvolvimento de aços inoxidáveis com efeito de memória de forma”, In: 50º Congresso Anual da ABM, São Pedro, SP. p.15-27.
- Otubo, J., Mei, P. R., Koshimizu, S., 1997, “Materiais com efeito de memória de forma: características principais e possíveis aplicações”, In: XIV Congresso Brasileiro de Engenharia Mecânica – COBEM, Bauru, SP.
- Otubo, J., Nascimento, F. C., Mei, P. R., Cardoso, L. P., Kaufman, M. J., 2002, “Influence of austenite grain size on mechanical properties of stainless SMA”, *Materials Transactions*, v.43, n.5, p.916-919.
- Otubo, J., Mei, P. R., Lima, N. B., Serna, M. M., Gallego, E., 2007, “O efeito do tamanho de grão austenítico no número de orientações das variantes de martensita em ligas inoxidáveis com efeito de memória de forma”, *Revista Escola de Minas, Ouro Preto, MG*. p.129-134.
- Otubo, J., Júnior, A.R., Neto, C.M., 2008, “Stainless SMA with damping capacity for aeronautical structures”, In: *Proceedings of the International Conference on Shape Memory and Superelastic Technologies*, Tsukuba, Japan, p.631-636.
- Sawaguchi, T., Ogawa, K., Kikuchi, T., 2008, “Absorption of seismic vibration by Fe-Mn-Si-based shape memory alloys and TRIP/TWIP steels”, In: *Proceedings of the International Conference on Shape Memory and Superelastic Technologies*, Tsukuba, Japan, p.637-644.
- Silva, C. E., Otubo, J., 2008, “Influência da temperatura de solubilização no tamanho de grão austenítico de ligas à base de Fe-Mn-Si com efeito de memória de forma: resultados preliminares”, In: 63º Congresso Anual da ABM, Santos, SP. p.2613-2621.

- Silva, C. E., Otubo, J., Rosato Júnior, A., 2008, “A influência do tempo e temperatura de austenitização e da composição química na microestrutura de ligas inoxidáveis com efeito de memória de forma”, In: IX Seminário Brasileiro do Aço Inoxidável – INOX’2008, São Paulo, SP. p.42-48.
- Silva, C. E., Rosato Júnior, A., Otubo, J., 2008, “The influence of austenitizing temperature and chemical composition on the microstructure of stainless shape memory steel”, In: 18° Congresso Brasileiro de Engenharia e Ciência dos Materiais – 18° CBECimat, Porto de Galinhas, PE. p.5875-5882.
- Silva, C. E., Otubo, J., 2009, “Influência da temperatura de austenitização na dureza, resistência à compressão e capacidade de recuperação de forma de ligas inoxidáveis”, In: 64° Congresso Anual da ABM, Belo Horizonte, MG.
- Wen, Y. H., Yan, M., Li, N., 2004, “Remarkable improvement of shape memory effect in Fe-Mn-Si-Cr-Ni-C alloy by ageing with deformation”, Scripta Materialia, 50, p.835-838.

## **6. RESPONSIBILITY NOTICE**

The authors are the only responsible for the printed material included in this paper.